A Fast Auto White Balance Scheme for Digital Pathology

Hrushikesh Garud[1], Ajoy K. Ray[2], Manjunatha Mahadevappa[3], Jyotirmoy Chatterjee[4] and Subhamoy Mandal[5]

***Abstract*—This paper presents a fast and accurate auto white balance scheme specifically suited for white balance (WB) correction in digital pathology applications. The scheme uses low-level statistics based technique for illuminant estimation and linear transformation method for image correction. The WB performance of the proposed scheme has been tested in various real life conditions and found to be within just noticeable difference of the ideal WB scenario.**

***Index Terms*—Color constancy, auto white balance, digital pathology, computer vision**

I. Introduction

Color constancy property of the vision system allows humans to perceive colors of objects as being essentially independent of the light which illuminates them [1]. Similarly, computational color constancy aims to estimate actual color in an acquired scene image disregarding the illuminant [2]. The algorithms and techniques used to attain color constancy in imaging systems have a common goal to render white objects as white under any light source [3] and are commonly referred to as gray balance or white balance (WB) techniques. Digital pathology systems which rely on comprehensive integration of digital imaging and bright-field microscopy systems inherit the limitations and problems of its constituent subsystems including the problem of noise corruption, non-uniform luminance, limited depth-of-field at high objective magnifications [4], image contrast [5] and computational color constancy.

The problem of computational color constancy is especially critical for anatomic pathology as differential staining of tissue and cellular components forms the basis for disease diagnosis both by human experts [6] and computer vision algorithms. But it has not been explored to the same extent for digital microscopy systems as it has been for consumer electronics applications [7], [8]. Only few approaches like blankfield correction [9], and auto white balance (AWB) method for digital microscope [10] have been used for color constancy. Blank-field approach though accurate needs manual setup and is not suitable for scenarios where scene illuminant is dynamic. The AWB method (Itr+GWA) proposed by Yan and others in [10] is a combination of iterative gray point detection method [11] and gray world method [12]. Where, the gray world assumption method provides coarse adjustment and iterative method provides fine adjustment. The Itr+GWA approach improves on the method proposed by Huo et al. in [11] by adding brightness constraint to the process of gray point detection and tile based selection thereof. Though robust and accurate, Itr+GWA approach requires cautious selection of multiple parameters in gray point detection method to obtain optimal qualitative performance. Further, choice of these parameters strongly affects the computational performance of the algorithm, which is already an iterative and computationally complex method involving color space conversion, image segmentation and correction operations. This renders the Itr+GWA approach unsuitable for real time applications.

Here we present a fast and accurate AWB scheme for application in digital pathology systems, where it can be used as primary method for WB correction or to correct images acquired with wrong white balance settings. The proposed AWB scheme uses combination of a static method of illuminant estimation [8] called White Patch Retinex (WPR)method [13], [14] and linear transformation model of WB correction of the images [15]. The WPR method, that has been designed to achieve color constancy under uniform illumination and is suitable for brightfield microscopy. Its advantages include- it does not require training data, is simpler to implement, and has a very low computational complexity. The linear model of WB correction operates only on two color channels, and thus further reduces computational complexity of the scheme. Additionally this method of WB correction does not introduce any significant change in image brightness as green channel, which contributes the most to the perception of brightness, is left unaltered. The WB performance of the proposed scheme has been validated on a set of pathological images. The WB performance is also compared with Itr+GWA method which has been previously used in digital microscopy applications.

Further, this paper is organized as follows. Section II presents overview and details of the proposed AWB scheme. Section III presents details of the experiments conducted to evaluate WB performance of the proposed scheme. Conclusions of the study are presented in sectionIV.

II. The Auto White Balance Scheme

The AWB techniques commonly estimate scene illuminant using acquired image itself and use this information to adjust

[1]H. Garud, is with School of Medical Science and Technology, IIT Kharagpur, Kharagpur 721 302, INDIA.
garudht@gmail.com
[2]A. K. Ray, is with Department of Electronics and Electrical Communication Engineering, IIT Kharagpur, Kharagpur 721 302, INDIA.
ajoy_ray2004@yahoo.com
[3]M. Manjunatha, is with School of Medical Science and Technology, IIT Kharagpur, Kharagpur 721 302, INDIA.
mmaha2@smst.iitkgp.ernet.in
[4]J. Chatterjee, is with School of Medical Science and Technology, IIT Kharagpur, Kharagpur 721 302, INDIA.
jchatterjee@smst.iitkgp.ernet.in
[5]S. Mandal, is with School of Medical Science and Technology, IIT Kharagpur, Kharagpur 721 302, INDIA.
smandal.biomed@gmail.com

978-1-4799-2131-7/14/$31.00 ©2014 IEEE

color intensities in the image to achieve color constancy [8]. Typical functional flow of the process is as follows

Illuminant estimation → WB parameter estimation → WB correction (image correction)

In the proposed AWB scheme, illuminant estimation is done by WPR technique [13], [14] followed by computation of correlated color temperature(CCT) [16]. The WB correction parameters are calculated as per requirements of the linear transformation model [15] used by WB correction stage. Details of these functional steps are presented in three parts as follows: illuminant estimation in section II-A, the gain and offset parameters computation in section II-B and the linear model of WB correction in section II-C.

A. Illuminant estimation

1) The White Patch Retinex Method: WPR a simplified version of the retinex algorithm [17], relies on having white patch somewhere in the image for estimation of the illuminant. The idea is, if there is a blank patch or the unstained portion of the tissue on parts of the slide in field of view, then this patch transmits the maximum light possible for each color channel, and hence represents the color of the illuminant. Instead of looking for white patches in the image, the WPR algorithm uses intensity k as an estimate of the illuminant such that all pixels with intensity higher than k account for some $p\%$ of total number of pixels in the image. For an image $\mathbf{f}$ of dimension $M \times N$ with L possible unique gray levels in range $[0,\ \mathrm{L}-1]$ estimate of illuminant in channel $c \in \{\text{red, green ,blue}\}$ is obtained as

$$\iota_c = k|_{\sum_{j=k}^{L-1} h_c(j) > \frac{pMN}{100} \text{ AND } \sum_{j=k+1}^{L-1} h_c(j) < \frac{pMN}{100}} \tag{1}$$

where h_c is histogram for color channel f_c and ι_c is in range $[0,\ \mathrm{L}-1]$. Such estimation of the illuminant is accurate when white patch(es) are present in the scene or if it has sufficiently diverse colors [18].

2) Correlated Color Temperature Estimation: Given color composition of the illuminant, corresponding CCT is estimated using model proposed by Hernández-Andrés et.al. [19]. This model takes illuminant color in the CIE 1931 XYZ color space as input and computes corresponding CCT as

$$\mathrm{CCT} = A_0 + A_1 e^{\frac{H}{t_1}} + A_2 e^{\frac{H}{t_2}} + A_3 e^{\frac{H}{t_3}} \tag{2}$$

where $H = -(x - x_e)/(y - y_e)$, x and y are chrominance values for the estimated illuminant $\{\boldsymbol{\iota} = \{\iota_c|\ c \in \{\text{red, green blue}\}$ in CIE 1931 XYZ color space and x_e, y_e, A_0, A_1, A_2, A_3, t_1, t_2, and t_3 are the model constants [19].

B. White balance parameter estimation

The linear model of image correction uses scale and shift operations on color values to obtain illuminant invariant description of the scene. Accordingly the gain factors can be defined as ratio of reference/canonical illuminant $\mathbf{I} = \{\mathrm{I}_c|c \in \{\text{red, green blue}\}\}$ to the estimated illuminant (ι_c) (see Eq.3)

$$\kappa_c = \frac{\mathrm{I}_c}{\iota_c} \tag{3}$$

and proposed AWB scheme defines $\mathbf{I}$ as

$$\mathrm{I}_c = \iota_{\text{green}}\ \forall c \in \{\text{red, green, blue}\} \tag{4}$$

And the offset values are calculated as

$$\tau_{\text{red}} = \max\left(1, \frac{CCT - CCT_{Ref}}{A}\right) \times (\kappa_{\text{red}} - 1) \tag{5}$$

$$\tau_{\text{green}} = 0$$

$$\tau_{\text{blue}} = \max\left(1, \frac{CCT_{Ref} - CCT}{A}\right) \times (\kappa_{\text{blue}} - 1)$$

Here CCT_{Ref} stands for CCT of the canonical/reference illuminant and $A(= 100)$ is a constant [19].

Now let $\boldsymbol{\kappa}$ and $\boldsymbol{\tau}$ be the diagonal transformation and column matrix representations for the *two* WB parameters (gain factors and offset) used in linear model applied in WB correction process, then they are defined as

$$\boldsymbol{\kappa} = \begin{bmatrix} \kappa_{\text{red}} & 0 & 0 \\ 0 & \kappa_{\text{green}} & 0 \\ 0 & 0 & \kappa_{\text{blue}} \end{bmatrix} \quad \text{and} \quad \boldsymbol{\tau} = \begin{bmatrix} \tau_{\text{red}} \\ \tau_{\text{green}} \\ \tau_{\text{blue}} \end{bmatrix} \tag{6}$$

C. White balance correction

In this step of the proposed and reference AWB schemes actual WB correction. For a pixel at a location (x, y) in the image $\mathbf{f}$ the WB correction process is defined as

$$\mathbf{f}_{wb}(x, y) = \boldsymbol{\kappa} \times \mathbf{f}(x, y) + \boldsymbol{\tau} \tag{7}$$

here $\mathbf{f}(x, y) = \begin{bmatrix} \mathrm{f}_{\text{red}}(x, y) & \mathrm{f}_{\text{green}}(x, y) & \mathrm{f}_{\text{blue}}(x, y) \end{bmatrix}^T$ and $\mathrm{f}_{\text{red}}(x, y)$, $\mathrm{f}_{\text{green}}(x, y)$ and $\mathrm{f}_{\text{blue}}(x, y)$ represent the gray scale values for three color channels and $\mathbf{f}_{wb}$ represents the white balanced output.

III. Experiments and Results

The proposed and reference AWB (Itr+GWA) schemes have been tested and evaluated on a database consisting 40 images of cytological and histological slides acquired using diagnostic pathology laboratory grade microscopes. The cameras connected with the microscopes are programmed to provide uncompressed, RGB coded image data without performing any WB correction or with wrong WB correction. Four sample inputs to the AWB algorithms and corresponding outputs obtained with two methods are shown in Fig. 1. Input images 1 and 4(Fig.1a and Fig.1j respectively) have been obtained with the microscope that uses LED illumination and images 2 and 3 (Fig.1d and Fig.1g respectively) have been obtained with the microscope that uses Halogen lamp for illumination. Both the AWB methods are seen to be performing well under simple and complex scene conditions.

The WB accuracy of an AWB scheme in digital pathology application can be measured as color error for true gray pixels corresponding to a blank patch or an unstained tissue section in the slide. The color error for a true gray pixel in an image is computed in the CIEL*a*b* color space where perceptible color difference is approximately equal to Euclidean distance in the color space. For given color values $\{L*,\ a*,\ b*\}$ of a true gray pixel and corresponding reference color values

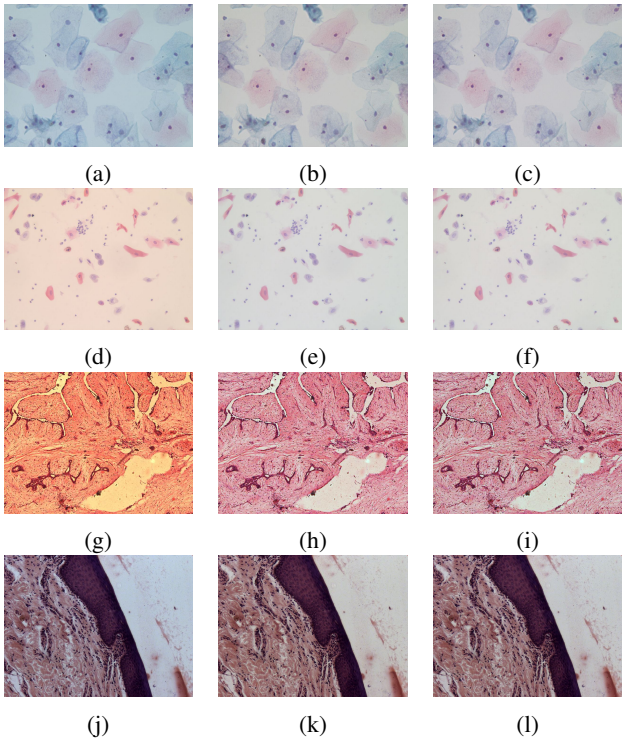

Fig. 1: {**(a), (d), (g),** and **(j)**} Input images to the AWB methods. {**(b), (e), (h)** and **(k)**} and {**(c), (f), (i),** and **(l)**}outputs of WPR based and Itr+GWA based AWB Schemes respectively.

$\{L^r*,\ a^r*,\ b^r*\}$ under ideal WB condition, the color error (omitting effect of exposure error) is defined as

$$E_{a*b*} = \sqrt{(\Delta a*)^2 + (\Delta b*)^2} \tag{8}$$

where $\Delta a* = a^r * - a*$, and $\Delta b* = b^r * - b$ [20]. Correct WB of the images should lead to color error smaller than that of the non-white balanced images and for perfect WB the error should be zero for white-balanced images.

Average pre-AWB color error for the input test set is 6.56. For the proposed AWB scheme the post-AWB color error becomes 1.98 ($p = 96.5\%$), which is well within the just noticeable difference(JND) [21] of the ideal WB scenario. The value of p that gives best performance for the proposed AWB scheme has been selected empirically by varying p in the range of 90 to 99%. Plot for average post-AWB color error versus p is shown in Fig.2. For the Itr+GWA based AWB scheme the post-AWB color error has been found to be 2.48 over same set of images. Plot of color error distributions in the dataset before and after AWB is shown in Fig.3. It can be observed that WPR method based AWB scheme performs consistently well in terms of reducing color error and is more precise.

From the results shown here in Fig. 1, 2 and 3 it can be observed that WPR method based AWB scheme performs consistently good in variety of digital pathology scenarios and provides accurate WB performance. It performs exceptionally well when blank patches are present in the scene

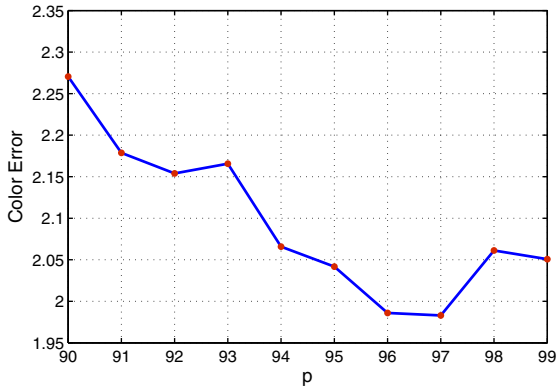

Fig. 2: Plot for average post-AWB color error for the WPR based AWB versus p

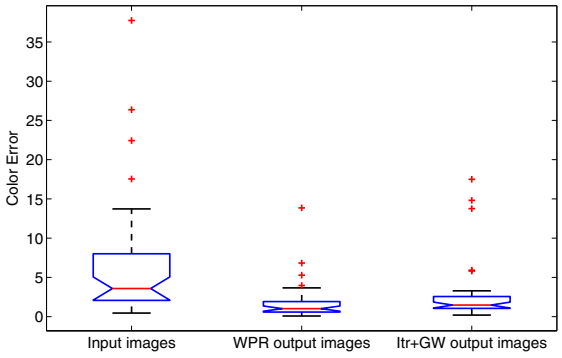

Fig. 3: Color error distributions in the dataset before and after AWB

or if the image has sufficiently diverse colors. Whereas GWA based AWB scheme performs poorly for the images which have low color diversity and can produce severe color artifacts in such images with color error very close to or higher than the input image color error.

IV. Conclusion

A scheme for WB correction in digital pathology applications is presented here. This method does not require training data, is simpler to implement and tune, and has a very low computational complexity. Testing of the proposed scheme under variety of digital pathology scenarios has shown it to provide WB performance at par with more complex existing method and accurate within JND of the ideal WB scenario. In conclusion the proposed system is promising as primary method for WB correction or to correct images acquired with wrong WB settings in digital pathology applications.

References

[1] G. Biernson, "A feedback-control model of human vision," *Proceedings of the IEEE*, vol. 54, no. 6, pp. 858–872, 1966.

[2] S. Bianco, G. Ciocca, C. Cusano, and R. Schettini, "Improving color constancy using indoor/outdoor image classification," *Image Processing, IEEE Transactions on*, vol. 17, no. 12, pp. 2381–2392, 2008.

[3] Y. Kim, J.-S. Lee, A. W. Morales, and S.-J. Ko, "A video camera system with enhanced zoom tracking and auto white balance," *Consumer Electronics, IEEE Transactions on*, vol. 48, no. 3, pp. 428–434, 2002.

[4] H. Garud, A. Ray, S. Mandal, D. Sheet, M. Mahadevappa, and J. Chatterjee, "Volume visualization approach for depth-of-field extension in digital pathology," in *Image and Signal Processing (CISP), 2011 4th International Congress on*, vol. 1, 2011, pp. 335–339.

[5] H. Garud, D. Sheet, A. Suveer, P. Karri, A. Ray, M. Mahadevappa, and J. Chatterjee, "Brightness preserving contrast enhancement in digital pathology," in *Image Information Processing (ICIIP), 2011 International Conference on*, 2011, pp. 1–5.

[6] A. C. Ruifrok and D. A. Johnston, "Quantification of histochemical staining by color deconvolution," *Analytical and quantitative Cytology and Histology*, vol. 23, pp. 291–299, 2003.

[7] K. Barnard, V. Cardei, and B. Funt, "A comparison of computational color constancy algorithms I: Methodology and experiments with synthesized data," *Image Processing, IEEE Transactions on*, vol. 11, no. 9, pp. 972–984, 2002.

[8] A. Gijsenij, T. Gevers, and J. van de Weijer, "Computational color constancy: Survey and experiments," *Image Processing, IEEE Transactions on*, vol. 20, no. 9, pp. 2475–2489, 2011.

[9] G. D. Marty, "Blank-field correction for achieving a uniform white background in brightfield digital photomicrographs," *Biotechniques*, vol. 42, pp. 716, 718, 720, 2007.

[10] X.-X. Yan, L. Zhang, T.-Y. Zhao, and F.-H. Yu, "The research on automatic white balance for digital microscope," vol. 7384, 2009, pp. 738 417–738 417–7.

[11] J. yan Huo, Y. lin Chang, J. Wang, and X. xia Wei, "Robust automatic white balance algorithm using gray color points in images," *Consumer Electronics, IEEE Transactions on*, vol. 52, no. 2, pp. 541–546, 2006.

[12] G. Buchsbaum, "A video camera system with enhanced zoom tracking and auto white balance," *J. Franklin Inst.*, vol. 310, no. 1, pp. 1–26, 1980.

[13] E. H. Land, "The retinex theory of color vision," *Scientific American*, vol. 237, no. 6, pp. 108–128, 1977.

[14] M. Ebner, *Algorithms for Color Constancy under Uniform Illumination*. John Wiley & Sons, Ltd, 2007, pp. 103–141.

[15] C.-L. Chen and S.-H. Lin, "Intelligent color temperature estimation using fuzzy neural network with application to automatic white balance," *Expert Systems with Applications*, vol. 38, no. 6, pp. 7718–7728, 2011.

[16] R. Davis, "A correlated color temperature for illuminants," *J. Res. Nat. Bur. Stand.*, vol. 7, no. 4, pp. 659–681, 1931.

[17] E. H. Land and J. J. McCann, "Lightness and retinex theory," *J. Opt. Soc. Am.*, vol. 61, no. 1, pp. 1–11, 1971.

[18] M. Ebner, "Combining white-patch retinex and the gray world assumption to achieve color constancy for multiple illuminants," in *Pattern Recognition*, ser. Lecture Notes in Computer Science, B. Michaelis and G. Krell, Eds. Springer Berlin Heidelberg, 2003, vol. 2781, pp. 60–67.

[19] J. Hernández-Andrés, R. L. Lee, and J. Romero, "Calculating correlated color temperatures across the entire gamut of daylight and skylight chromaticities," *Appl. Opt.*, vol. 38, no. 27, pp. 5703–5709, 1999.

[20] G. Sharma and H. Trussell, "Digital color imaging," *Image Processing, IEEE Transactions on*, vol. 6, no. 7, pp. 901–932, 1997.

[21] M. Mahy, L. V. Eycken, and A. Oosterlinck, "Evaluation of uniform color spaces developed after the adoption of CIELAB and CIELUV," *Color Research and Application*, vol. 19, pp. 105–121, 1994.